Current Biology 17, 1721–1734, October 23, 2007 ©2007 Elsevier Ltd All rights reserved DOI 10.1016/j.cub.2007.09.028

Article

# Zebrafish Melanophilin Facilitates Melanosome Dispersion by Regulating Dynein

**Lavinia Sheets,[1] David G. Ransom,[1] Eve M. Mellgren,[2] Stephen L. Johnson,[2] and Bruce J. Schnapp[1,*]**

[1]Department of Cell and Developmental Biology
Oregon Health and Science University
Basic Science Building Room 5365
3181 SW Sam Jackson Park Road
Portland, Oregon 97201-3098

[2]Department of Genetics
Washington University School of Medicine
St. Louis, Missouri 63110

## Summary

**Background:** Fish melanocytes aggregate or disperse their melanosomes in response to the level of intracellular cAMP. The role of cAMP is to regulate both melanosome travel along microtubules and their transfer between microtubules and actin. The factors that are downstream of cAMP and that directly modulate the motors responsible for melanosome transport are not known. To identify these factors, we are characterizing melanosome transport mutants in zebrafish.

**Results:** We report that a mutation (allele *j120*) in the gene encoding zebrafish melanophilin (Mlpha) interferes with melanosome dispersion downstream of cAMP. Based on mouse genetics, the current model of melanophilin function is that melanophilin links myosin V to melanosomes. The residues responsible for this function are conserved in the zebrafish ortholog. However, if linking myosin V to melanosomes was Mlpha's sole function, elevated cAMP would cause *mlpha*$^{j120}$ mutant melanocytes to hyperdisperse their melanosomes. Yet this is not what we observe. Instead, mutant melanocytes disperse their melanosomes much more slowly than normal and less than halfway to the cell margin. This defect is caused by a failure to suppress minus-end (dynein) motility along microtubules, as shown by tracking individual melanosomes. Disrupting the actin cytoskeleton, which causes wild-type melanocytes to hyperdisperse their melanosomes, does not affect dispersion in mutant melanocytes. Therefore, Mlpha regulates dynein independently of its putative linkage to myosin V.

**Conclusions:** We propose that cAMP-induced melanosome dispersion depends on the actin-independent suppression of dynein by Mlpha and that Mlpha coordinates the early outward movement of melanosomes along microtubules and their later transfer to actin filaments.

## Introduction

Fish and amphibians constantly adjust their pigmentation in order to blend with backgrounds that vary from light to dark. Specialized cells, called melanocytes, accomplish this by either aggregating or dispersing their membrane-bound pigment granules, called melanosomes, depending on the level of intracellular cAMP. Although these cells have been used for many years for investigating intracellular transport regulation [1], it is not understood how cAMP regulates the molecular motors responsible for melanosome transport. Here, we have used zebrafish to identify and characterize a gene product that regulates melanosome motors downstream of cAMP.

Melanocyte microtubules are arrayed with their minus ends at the cell center; hence, the minus-end motor cytoplasmic dynein carries melanosomes inward, leading to aggregation [2, 3], whereas the plus-end motor kinesin-2 carries melanosomes outward, leading to dispersion [4]. Melanosomes also interact with myosin V, which switches their transport from microtubules to actin filaments [2, 5, 6]. If the transfer to actin is inhibited in fish melanocytes, e.g., by disassembling the actin cytoskeleton, melanosomes fail to disperse evenly. Instead, they "hyperdisperse"; they move to the minus ends of microtubules without getting off and thereby accumulate at the cell periphery, leaving most of the cell pigment free [2]. To establish an even distribution of melanosomes during dispersion, melanocytes must coordinate transport between microtubules and actin precisely.

Although melanosomes aggregate and disperse globally, the motion of individual melansomes is saltatory and bidirectional. Episodes of travel in each direction are interspersed with each other and with periods of undirected motion. The switch from linear motion to a period of undirected motion reflects a switch in the transfer of the melanosome from microtubules to actin filaments [2, 7, 8]. Biasing the persistence of dynein- versus kinesin-driven motility episodes is what leads to global aggregation or dispersion [7, 9]. These or similar mechanisms presumably operate in other cells to regulate the bidirectional transport of other cargoes, including chromosomes on the mitotic spindle [10] and many organelles in neurons and other cells [11]. Most cells also coordinate microtubule- and actin-based transport; e.g., post-Golgi transport vesicles destined for the plasma membrane must leave microtubules and penetrate the cortical actin network in order to reach their final destinations [12].

A significant advantage of fish melanocytes for investigating these aspects of motor regulation is that melanosome transport is regulated by the level of intracellular cAMP. Melanin stimulating hormone (MSH) elicits a cAMP increase that activates protein kinase A (PKA), leading to melanosome dispersion, whereas melanin concentrating hormone (MCH) elicits a cAMP decrease, which enhances the phosphatase activity that reverses PKA-dependent phosphorylation, leading to melanosome aggregation [9, 13, 14]. The current model for how cAMP levels regulate melanosome motor activities is based on analyses of single-melanosome movements in black tetra fish [9] and *Xenopus* [7] melanocytes. In

*Correspondence: schnappb@ohsu.edu

Table 1. Pharmacological Analysis of Melanosome Transport in Wild Type Zebrafish Melanocytes

| Reagent | Mechanism | Effect |
|---|---|---|
| α-MSH (0.2–20 μM) | Activates adenylyl cyclase via Gs-protein coupled receptor | Dispersion |
| MCH (0.1–1.0 μM) | Inhibits adenylyl cyclase via Gi-protein coupled receptor | Aggregation |
| Caffeine (5 mM) | A1 adenosine receptor antagonist; elevates intracellular cAMP | Dispersion |
| Epinephrine (0.1 mM) | A2-adrenergic receptor agonist; inhibits adenylyl cyclase via Gi-protein coupled receptor | Aggregation |
| Forskolin (200 μM) | Adenylyl cyclase activator | Dispersion |
| sp-cAMP (30 μM) | Membrane permeable cAMP analog | Dispersion |
| SQ 22,536 (100 μM–1 mM) | Adenylyl cyclase inhibitor | Inhibits dispersion |
| Okadaic Acid (1 μM) | Serine/threonine phosphatase inhibitor | Inhibits aggregation |
| Cyclosporin A (20 μM) | Protein phosphatase 2B inhibitor | No effect |
| H-89 (40 μM) | Protein kinase A inhibitor | Aggregation |

To verify that the cAMP signaling pathways that regulate melanosome transport in other fish species [9, 14, 38] also do so in zebrafish, we exposed cultured melanocytes to reagents that activate or inhibit known players in the signaling pathways. The effects of these reagents on zebrafish melanocytes confirm the importance of cAMP modulation and the activity of PKA and a phosphatase in the regulation of zebrafish melanosome movement and suggest that the overall pathways that regulate dispersion and aggregation in zebrafish are similar to what has been established in other species of fish.

response to MSH, cAMP levels at first rise and then decline. These kinetics correlate with those of plus-end travel, and this implies that PKA phosphorylation of an as yet unknown protein leads to changes in the activity of kinesin-2. As cAMP and plus-end travel decline, the frequency of minus-end motility episodes increases. This leads to a rise in actin-based movement because melanosomes switch their transport from microtubules to actin during dynein motility events [7, 9]. The model is that myosin V and cytoplasmic dynein are in a tug of war, which myosin V wins [7].

The switch from aggregation to dispersion upon exposing melanocytes to MSH entails the suppression of dynein activity [7, 9]. The molecular mechanism underlying this suppression of dynein is not understood. Analyses of single-melanosome velocities in latrunculin-treated melanocytes, which lack actin filaments, suggest that the rise in PKA activity at the onset of dispersion might reduce the number of active dyneins on the melanosome [15], independently of myosin V and actin. However, because the tug of war with myosin V is capable of shortening the persistence of dynein motility episodes [7], this might also contribute to the suppression of dynein at the onset of dispersion.

For understanding how cAMP modulates melanosome transport, it would be helpful to identify the molecules that function between cAMP and the melanosome motors. Here, we identify one of these molecules through the analysis of the zebrafish pigment mutant allele *j120*. Our studies suggest that microtubule-to-actin transfer of melanosomes might involve more than simply attaching a myosin to the organelle. Our findings support models wherein microtubule-to-actin transfer occurs through linked regulation of both microtubule- and actin-motor activities.

## Results

### The Mutation *j120* Interferes with Melanosome Dispersion Downstream of cAMP

We identified the recessive mutant allele *j120* through an ENU mutagenesis screen. *j120* homozygous fish are viable and appear normal apart from an inability to adapt their pigmentation to a dark background. Like other fish, wild-type zebrafish aggregate and disperse their melanosomes in response to MCH and MSH, respectively (Table 1; Figure S1 in the Supplemental Data available online). The *j120* mutant fish appear normal when incubated in MCH, but upon exposure to MSH, the spots of pigment in the mutant remain small, whereas those in wild-type fish expand dramatically (Figure 1A). This indicates that the *j120* mutation interferes with melanosome dispersion.

To evaluate in more detail this melanosome transport defect, we cultured melanocytes from wild-type or *j120* mutant fish and used differential interference contrast microscopy to image and make movies of their melanosome movements (Figure 1B). After perfusion into the microscopy flow cell of a hormone or agonist that elicits melanosome aggregation (MCH or epinephrine) or dispersion (MSH or caffeine), we measured the time course of pigment contraction or expansion within individual cells (Figures 1B–1D). Melanocytes from *j120* mutant fish aggregate their melanosomes with the same kinetics as those of wild-type fish (Figures 1B and 1C) but disperse their melanosomes much more slowly than wild-type melanocytes (Figure 1D). In addition, whereas melanosomes in wild-type melanocytes spread to the cell margin within 5 min of applying dispersion-inducing drugs (Figures 1B–1D), the spreading of melanosomes in *j120* mutant melanocytes plateaus at 5–8 min with less than half of the projected cell area filled with melanosomes (Figures 1B–1D), a condition we refer to as partial dispersion.

We performed pharmacological experiments (Figures 1E and 1F; Table 1) to address whether the abnormal melanosome dispersion evident in *j120* melanocytes is a consequence of defective signaling through the MSH and G protein-dependent pathway that normally elicits dispersion by elevating intracellular cAMP [14]. Drugs that elevate intracellular cAMP artificially, including the activator of adenylyl cyclase, forskolin, and a membrane permeable analog of cAMP, sp-cAMP, elicit full dispersion in wild-type melanocytes (Figure 1E), and yet they have no effect on the slow and partial melanosome dispersion that marks *j120* melanocytes (Table 1, Figure 1E). Therefore, the defect in *j120* melanocytes does not occur between MSH binding to its receptor and cAMP elevation.

To address whether elevated activity of the opposing phosphatase is responsible for the slow and partial melanosome dispersion in the mutant, we exposed wild-type and *j120* mutant melanocytes to 0.1 μM of the phosphatase inhibitor okadaic acid (Figure 1F). This treatment blocks melanosome aggregation in wild-type and *j120* mutant melanocytes (Figure 1F), consistent with inhibition of the phosphatase opposing PKA phosphorylation. However, this treatment does not rescue the partial dispersion phenotype of *j120* mutant melanocytes. Whereas wild-type melanocytes pretreated overnight with okadaic acid and then exposed to forskolin spread their melanosomes to the cell margin, the melanosomes within similarly treated *j120* melanocytes spread only part of the way to the cell periphery (Figure 1F).

Collectively, these pharmacological experiments indicate that the abnormal melanosome dispersion in *j120* mutant melanocytes is not due to abnormal signaling through cAMP- and PKA-dependent phosphorylation.

### Partial Dispersion in *j120* Mutant Melanocytes Is Independent of Actin

To address the possibility that partial melanosome dispersion in *j120* mutant melanocytes is caused by an abnormal microtubule or actin cytoskeleton, we visualized actin filaments and microtubules within melanocytes by antitubulin immunofluorescence and rhodamine-phalloidin labeling (Figure 2A). The microtubule and actin cytoskeletons of *j120* melanocytes appear indistinguishable from those of wild-type melanocytes. Thus, the partial dispersion of melanosomes in *j120* melanocytes cannot be attributed to a failure of microtubules to reach the cell periphery or to restriction of the melanocyte's actin filaments to the cell center.

To address whether the slow and partial melanosome transport in *j120* mutants is caused by premature transfer of melanosomes from microtubules to actin early in dispersion, we treated melanocytes with latrunculin A, which disassembles actin filaments (Figure 2B). In the presence of latrunculin, wild-type melanocytes respond to MSH or caffeine by hyperdispersing their melanosomes to the cell margin (Figure 2B), and such a response confirms earlier work in a different species of fish [2]. By contrast, latrunculin has no effect on the slow and partial dispersion of melanosomes in *j120* melanocytes (Figure 2B). Thus, the melanosome dispersion that persists in *j120* mutant melanocytes is independent of actin.

### Microtubule-Based Transport Underlies Melanosome Dispersion in *j120* Melanocytes

We addressed whether the spreading of melanosomes during MSH-induced dispersion in *j120* melanocytes occurs through the transport of individual melanosomes along microtubules, as in wild-type melanocytes [2, 7–9]. The alternative possibility would have been that melanosomes in *j120* melanocytes fail to load onto microtubules and that they spread through diffusion or a change in cell shape. To distinguish microtubule-based transport from other modes of spreading, we ascertained whether individual melanosomes in the mutant move along linear paths. According to previous studies [2], this would imply they are transported along microtubules. One difficulty was that the partial dispersion that marks *j120* melanocytes makes it difficult to identify the movements of individual melanosomes through stacks of sequential images. We therefore examined the sum of difference images, which we created by subtracting the previous frame from each new frame [16]. Summing sequences of difference images reveals only those objects that have moved and makes linear trajectories noticeable (Figure 1B). Our analyses reveal that many melanosomes in *j120* melanocytes execute bidirectional linear movements (Figure 1B, inset). We conclude that melanosomes in *j120* mutant melanocytes do not spread by diffusion, nor are they "stuck" together or stalled on microtubules. Instead, this analysis indicates that they spread by loading onto and moving along microtubules.

### The *j120* Mutation Prevents the Suppression of Minus-End Travel Episodes during Dispersion

The finding that during dispersion, some melanosomes in the *j120* mutant melanocytes translocate away from the main mass (Figure 1B, inset sequence) suggested we can analyze the kinetics of their movements to understand further how the mutation impacts the regulation of melanosome transport along microtubules. The motion of individual melanosomes is normally bidirectional, with a bias toward minus- or plus-end travel depending on whether the population as a whole is aggregating or dispersing [7, 9] (Figures 1B and 3). An attenuated rate of dispersion such as that seen in *j120* mutant melanocytes could result from either abnormally low plus-end travel or abnormally high minus-end travel. To address which of these two possibilities underlies the *j120* mutant phenotype, we tracked the movements of individual melanosomes, and from these tracks, we computed the average kinetic parameters of plus- and minus-end travel (Figure 3).

We tracked single melanosomes (Figure 3 and Table 2) for 30 s at 1.5 and 3 min after applying the stimulus to disperse (MSH or caffeine). Melanosome tracks (Figure 3A) show episodes of continuous outward (plus-end) or inward (minus-end) movements whose trajectories resemble those of immunostained microtubules. These episodes are interspersed with pause or random-motion periods, which we infer reflect a stopped state on the microtubule or actin-based transport. We treated pause or random-motion episodes as a single motion category ("undirected motion"). Previous studies of black tetra fish and *Xenopus* melanocytes have documented that linear- and random-motion components, virtually identical to those we report here, reflect microtubule- and actin-based transport, respectively [2, 7, 9].

We first compared wild-type and *j120* melanosome tracks with respect to the fraction of time (dwell time) melanosomes spend in the three motion categories. To compute dwell times, we pooled all tracks for wild-type or *j120* mutant melanosomes (Figure 3B). This analysis indicates that both wild-type and *j120* mutant melanosomes spend the majority of their time engaged in undirected motion, even as they disperse globally. *j120* mutant melanocytes differ from the wild-type in that their melanosomes engage in undirected motion less often (73% versus 79% of the time at 1.5 min; 66% versus 80% at 3 min) but engage in minus-end

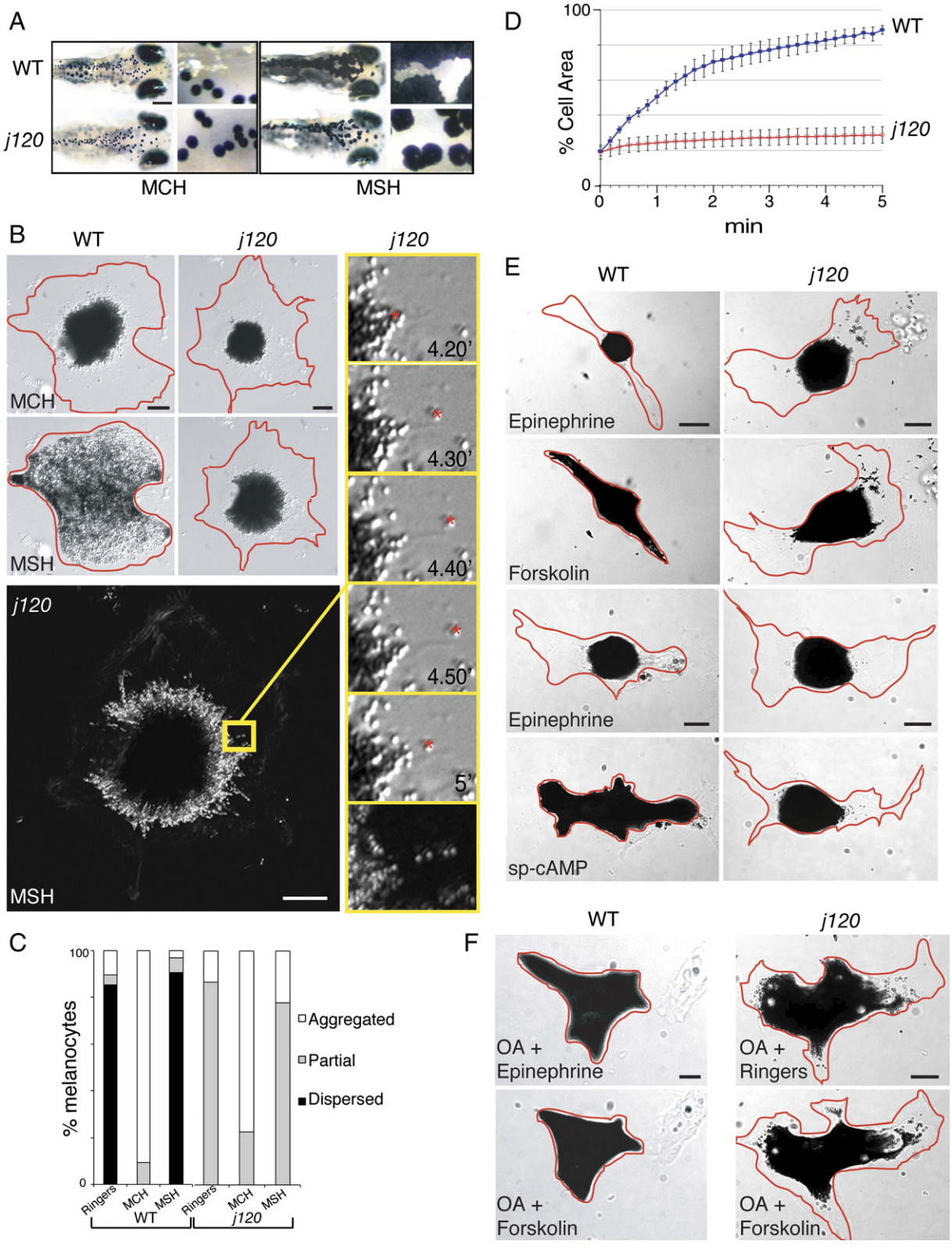


Figure 1. Characterization of Melanosome Transport in Wild-Type and *j120* Zebrafish Melanocytes

(A) Aggregation and dispersion in wild-type and mutant five-day-old larvae. In response to MCH, pigment appears similarly aggregated in mutant and wild-type fish. In response to MSH, melanocytes within wild-type fish disperse their pigment fully, whereas melanocytes in *j120* mutant fish do not. (The scale bar represents 200 μm in main images and 50 μm in insets.)

(B) Aggregation and dispersion in cultured wild-type and *j120* mutant melanocytes visualized by DIC microscopy. As shown in the top row, wild-type and mutant melanocytes fully aggregate their melanosomes after 5 min in MCH. Aggregation appears normal in the mutant melanocyte.

travel correspondingly more often (12% versus 3% at 1.5 min; 16% versus 5% at 3 min). Thus, the percentage of time melanosomes engage in plus-end travel is very similar between *j120* and wild-type melanocytes (15% versus 18% at 1.5 min; 18% versus 15% at 3 min). These findings suggest that excess minus-end travel might explain the slow dispersion of melanosomes in *j120* mutant melanocytes.

To measure plus- and minus-end travel along microtubules, we analyzed the microtubule-based components of the melanosome tracks from the dispersion-stimulated cells. We computed for each direction of movement and across all movement episodes the mean frequency of occurrence and the mean distance traveled (persistence) (Table 2). The product of mean frequency and mean persistence is the mean travel distance (d) that a melanosome moves in that direction (Figure 3C). On average, *j120* mutant and wild-type melanosomes travel similar distances toward microtubule plus ends (1.5 μm versus 1.3 μm at 1.5 min; 1.4 μm versus 1.1 μm at 3 min). In contrast, *j120* mutant melanosomes travel much farther than wild-type toward microtubule minus ends (1.2 μm versus 0.2 μm at 1.5 min; 1.6 μm versus 0.3 μm at 3 min). The abnormally high minus-end travel of *j120* melanosomes is caused by significant increases in both the frequency and persistence of minus-end motility episodes (Table 2). Persistence frequency distributions, which are described by the sum of two decaying exponentials, reflecting short and long classes of travel episodes [7, 17] (Figure S2) indicate that an excess of long episodes is predominantly responsible for elevating the mean persistence of minus-end melanosome motility in *j120* melanocytes.

In summary, the ratios of mean plus- to minus-end travel at the two time points are ~6:1 and 4:1 for wild-type, consistent with rapid global dispersion, whereas the *j120* ratios are ~1:1. We therefore conclude that in wild-type melanocytes, the function of the normal *j120* gene product is to suppress minus-end travel during dispersion and that this is essential for driving the rapid outward spreading of the melanosome population as a whole. This suppression of minus-end-directed travel in response to the dispersion stimulus does not occur in *j120* mutant melanocytes. The observation that minus-end travel is suppressed during dispersion in wild-type zebrafish melanocytes agrees with previous studies of black tetra fish and *Xenopus* melanocytes, which likewise show that the shift from aggregation to dispersion entails a decrease in minus-end travel [7, 9].

With respect to the kinetic parameters that underlie travel (frequency and persistence), comparisons between wild-type and *j120* melanocytes reveal additional facets about microtubule motor coordination. Between the 1.5 and 3 min time points, the average travel in the plus- and minus-end directions do not change dramatically. This is true for wild-type and *j120* melanocytes (Figure 3C). However, as a result of the mutation in *j120*, both the average frequency and persistence undergo sizeable changes over time (Table 2); these changes compensate so that for each direction, travel is constant. For plus-end travel, the average frequency increases ~2-fold (3.5 versus 6.0; Student's t test, $p < 0.020$) as the average persistence decreases by ~1/2 (0.43 μm versus 0.23 μm; $p < 0.0001$). On the contrary, for minus-end travel, the frequency again increases by ~2-fold (3.0 versus 5.7; $p < 0.007$), as the persistence decreases (0.40 versus 0.29 μm; $p < 0.14$). This is in contrast to wild-type melanocytes, for which frequency and persistence do not change significantly between the 1.5 and 3 min either for plus-end (4.2 versus 4.1 events in 30 s with average persistence 0.32 versus 0.27 μm) or minus-end travel (1.5 versus 1.9 events in 30 s with average persistence 0.13 versus 0.16 μm). Thus, the *j120* mutation unmasks a novel property of the motor coordination

As shown in the second row, exposure to MSH for 5 min elicits complete dispersion in wild-type but only partial dispersion in mutant melanocytes. The bottom and right-hand column contains a *j120* mutant melanocyte showing that during dispersion its melanosomes load on microtubules and move bidirectionally. Digital images of this melanocyte were collected over a 5 min period after the initiation of dispersion by MSH. Each preceding frame was subtracted from each new frame so that a difference image could be created, and the stack of difference images was summed through the recording period. Thus, this figure reveals the sum of what has moved during the recording period. Linear trajectories of many individual melanosomes are evident as white "beads on a string." One of these is within the area outlined in yellow. This area is shown at higher magnification at the bottom of the column of frames to the right. The upper five frames in the column show the direct images of the moving melanosome that produced the linear trajectory in the summed difference image. This melanosome moves bidirectionally (Scale bars represent 10 μm.).

(C) Fraction of cultured wild-type and *j120* mutant melanocytes that respond to hormones fully or partially. Melanocyte cultures were treated for 10 min with 0.5 μM MSH or 1 μM MCH. Partial dispersion (defined as melanosomes that spread from the aggregated state but did not completely fill the melanocyte within 10 min) or no dispersion (defined as melanosomes that remained aggregated after the dispersion stimulus) was evident in a minor fraction of wild-type melanocytes. *j120* homozygous mutant melanocytes were never observed to fully disperse their melanosomes ($n = 96$ and 75 for wild-type and mutant, respectively).

(D) Kinetics of global melanosome dispersion in cultured wild-type and mutant melanocytes. Wild-type and mutant melanocytes with melanosomes aggregated were stimulated to disperse with MSH or caffeine, and the percent of the projected cell area filled with melanosomes was measured at 10 s intervals. Data points are averages from five mutant and five wild-type melanocytes. (Error bars represent SEM.)

(E) Images of cultured wild-type and mutant melanocytes 5 min after applying compounds that lower or elevate intracellular cAMP levels. As shown in the first and third rows, melanocytes were first exposed to 0.1 mM epinephrine for aggregation induction. As shown in the second and fourth rows, melanocytes were then exposed to forskolin (200 μM) or sp-cAMP (30 μM). Both elicit full melanosome dispersion in the wild-type but only slow partial dispersion in the mutant.

(F) Response of cultured wild-type and *j120* mutant melanocytes to melanosome aggregation- and dispersion-inducing drugs applied after overnight pretreatment with the phosphatase inhibitor okadaic acid (OA). The top left contains the positive control showing that OA inhibits the phosphatase responsible for aggregation. Pretreatment of wild-type cultures with 1 μM OA inhibits aggregation induced by epinephrine. As shown in the top and bottom right images, overnight pretreatment of *j120* mutant melanocytes with 1 μM OA did not rescue partial dispersion, either in Ringers (upper) or after exposure to forskolin (lower). The small expansion of melanosomes in the *j120* mutant melanocyte in (F) compared to those in (E) is a side effect of the overnight exposure to okadaic acid. The main point is that forskolin does not induce further expansion to the cell periphery, as it does in wild-type melanocytes. As shown in the bottom left panel, forskolin induces full dispersion in wild-type melanocytes pre-treated with 1 μM OA. (Scale bars represent 10 μm.)

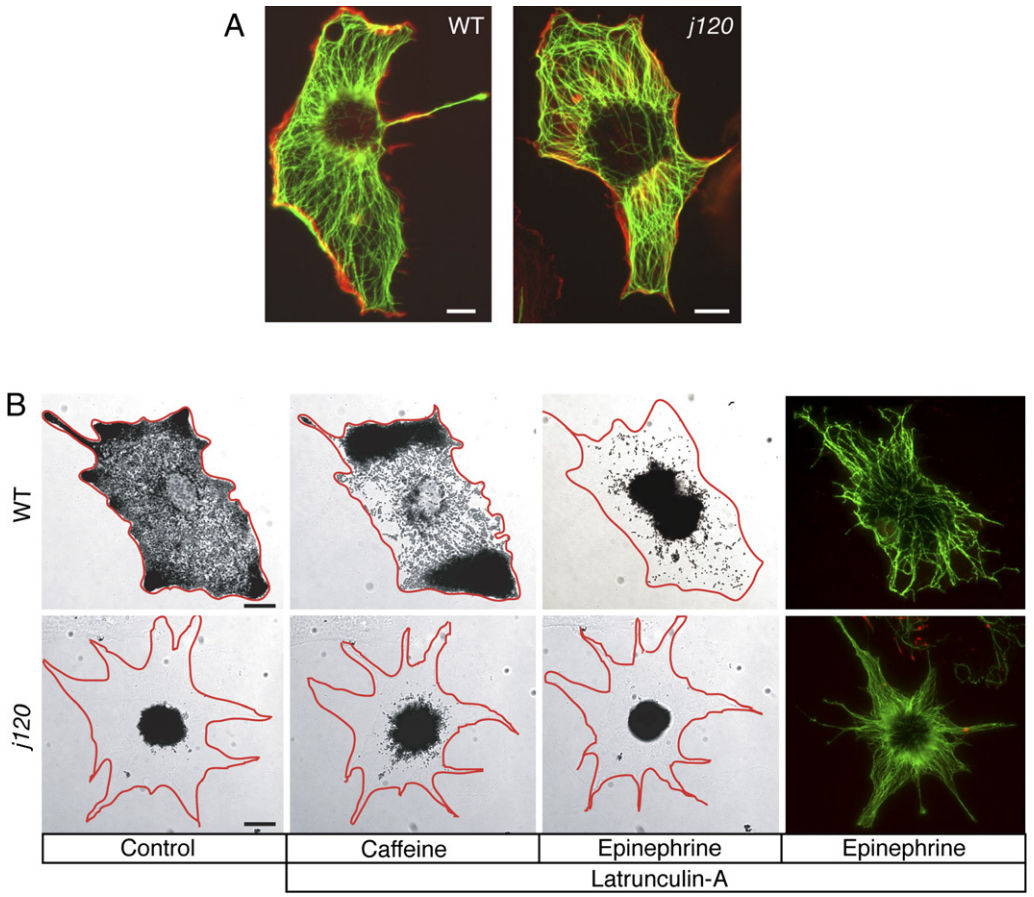


Figure 2. Partial Dispersion in *j120* Melanocytes Does Not Involve an Abnormal Microtubule or Actin Cytoskeleton and Is Independent of Actin

(A) Fluorescent images of rhodamine-phalloidin-labeled actin (red) and immuno-labeled α-tubulin (green) in cultured wild-type and *j120* mutant melanocytes. Microtubule and actin cytoskeletons appear normal in the mutant.

(B) Aggregation and dispersion of melanosomes in the absence of actin filaments. Melanocytes were treated with 5 μM latrunculin A for 15 min for disruption of actin filaments and then with caffeine for inducing dispersion. In latrunculin, wild-type melanocytes hyperdisperse their melanosomes, whereas the *j120* mutant melanocyte still only partially dispersed its melanosomes. Aggregation (induced by epinephrine) is unaffected by latrunculin. Rhodamine-phalloidin staining confirms the loss of actin filaments in the latrunculin-treated melanocytes. Microtubules (green) were labeled with an antibody against α-tubulin. (Scale bars represent 10 μm.)

machinery, which is that plus- and minus-end travel distances are regulated—through changes to the frequency and/or persistence of motility episodes—so that they balance, on average (Figure 3C). The normal function of the *j120* gene product is to upset this balance between plus- and minus-end travel (by suppressing the minus-end motor) in response to the dispersion stimulus.

### The *j120* Gene Is the Zebrafish Ortholog of Melanophilin

To shed light on how the *j120* gene product regulates melanosome motor activities, we characterized the molecular basis of the mutation. We mapped the gene to chromosome 6, to within 0.16 cM (0 crossovers in 1208 meioses) of an SSLP marker developed from BAC sequence BX649631 (Figure 4A). Because the ratio of physical to genetic distance in zebrafish is approximately 600 Kb/cM, this indicates that our tightly linked marker might be within 100 Kb of the *j120* mutation. Accordingly, we examined a region 100 Kb on either side of our marker for candidate genes. Among six genes evident within this interval, the only one with a known relationship to melanosome transport is a predicted melanophilin ortholog, which we henceforth refer to as *mlpha*. This acknowledges that zebrafish have a duplicate gene, which we refer to as *mlphb* (see below).

In mouse and human, melanophilin is genetically required for the accumulation of melanosomes at the dendritic tips of melanocytes [18–20]. Furthermore, although mammalian melanocytes differ from those of fish and frogs in that they do not engage in synchronous aggregation and dispersion of their melanosomes in response to cAMP, the mouse melanophilin mutant phenotype, called *leaden* [18], is nonetheless similar to that of *j120* in zebrafish: In both cases, melanosomes are clustered in the cell center and not dispersed throughout the cell.

To further explore whether *j120* is a mutation in the *mlpha* gene, we compared the sequence of wild-type *mlpha* cDNA with that of the mutant *mlpha*$^{j120}$ cDNA. We obtained cDNAs by performing RT-PCR on mRNA isolated from wild-type or homozygous mutant larvae. This comparison reveals that the *mlpha* transcript from

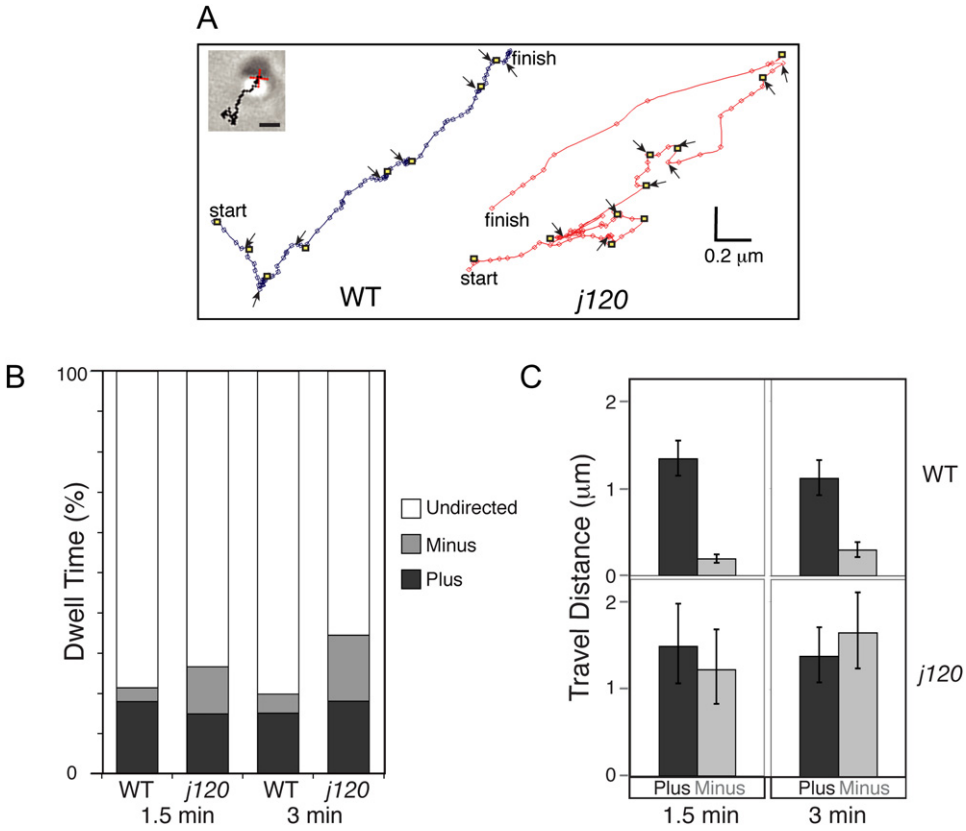


Figure 3. Analysis of Individual Melanosome Movements during Dispersion

(A) Melanosome tracks from wild-type and *j120* mutant melanocytes undergoing global dispersion. Track duration is 30 s; lines connect the successive positions. Yellow squares mark the start of directed travel along microtubules; black arrows mark periods of pause or undirected movement. Shown in the inset are the DIC image and track overlay for the wild-type melanosome. (The scale bar represents 1 μm.)

(B) Fraction of time melanosomes engage in the three motion states (minus-end, plus-end, or paused/undirected) during 30 s observation periods made 1.5 and 3 min after inducing dispersion. Each bar pools the data from all tracked melanosomes (Table 2) in the indicated category (e.g., wild-type, 1.5 min). The principal difference between the wild-type and mutant is that the mutant spends more time engaged in travel to the minus end.

(C) Microtubule plus- and minus-end travel of wild-type and *j120* melanosomes during 30 s observation intervals 1.5 and 3 min after initiating dispersion. Each bar represents the mean ± SEM over all tracked melanosomes. Travel distances are the products of the average run lengths and episode frequencies indicated in Table 2. Whereas for wild-type melanosomes plus-end travel exceeds minus-end travel, for mutant melanosomes, travel in the two directions is balanced.

*j120* mutants is misspliced such that it lacks the beginning of exon 7. This places the remaining 3′ portion of the transcript in the wrong reading frame and thus results in a premature stop codon that would truncate the protein after residue 238 (Figure 4B). This is consistent with the *mlpha*$^{j120}$ genomic DNA sequence, which reveals a point mutation in the exon 7 splice acceptor site (Figure 4C). As predicted, RT-PCR assays reveal

Table 2. Mean Kinetic Parameters of Microtubule-Based Travel

| | Wild-Type | Wild-Type | *j120* | *j120* | Wild-Type | Wild-Type | *j120* | *j120* |
|---|---|---|---|---|---|---|---|---|
| Travel direction | Plus-end | Plus-end | Plus-end | Plus-end | Minus-end | Minus-end | Minus-end | Minus-end |
| Time after dispersion stimulus (min) | 1.5 | 3 | 1.5 | 3 | 1.5 | 3 | 1.5 | 3 |
| Persistence of episodes (μm) (mean ± SEM) | 0.32 (±0.02) | 0.27 (±0.02) | 0.43 (±0.05) | 0.23 (±0.02) | 0.13 (±0.01) | 0.16 (±0.02) | 0.40** (±0.06) | 0.29* (±0.04) |
| Number of episodes in 30 s (mean ± SEM) | 4.2 (±0.5) | 4.1 (±0.4) | 3.5 (±0.7) | 6.0* (±0.8) | 1.5 (±0.3) | 1.9 (±0.3) | 3.0* (±0.6) | 5.7** (±0.7) |
| Number of melanocytes observed | 5 | 5 | 4 | 4 | 5 | 5 | 4 | 4 |
| Number of melanosomes tracked | 86 | 76 | 36 | 39 | 86 | 76 | 36 | 39 |

The table shows the average number of plus- and minus-end motility episodes and their average persistence during 30 s observation periods 1.5 and 3 min after the dispersion stimulus. The mean frequency of minus-end episodes and their mean distance (persistence) are significantly different between the wild-type and *j120* mutants at both 1.5 and 3 min after the initiation of dispersion. In addition, the mean frequency of plus-end episodes are significantly different between the wild-type and *j120* mutants at 3 min (unpaired Student's t test: **p < 0.0001; *p < 0.05).

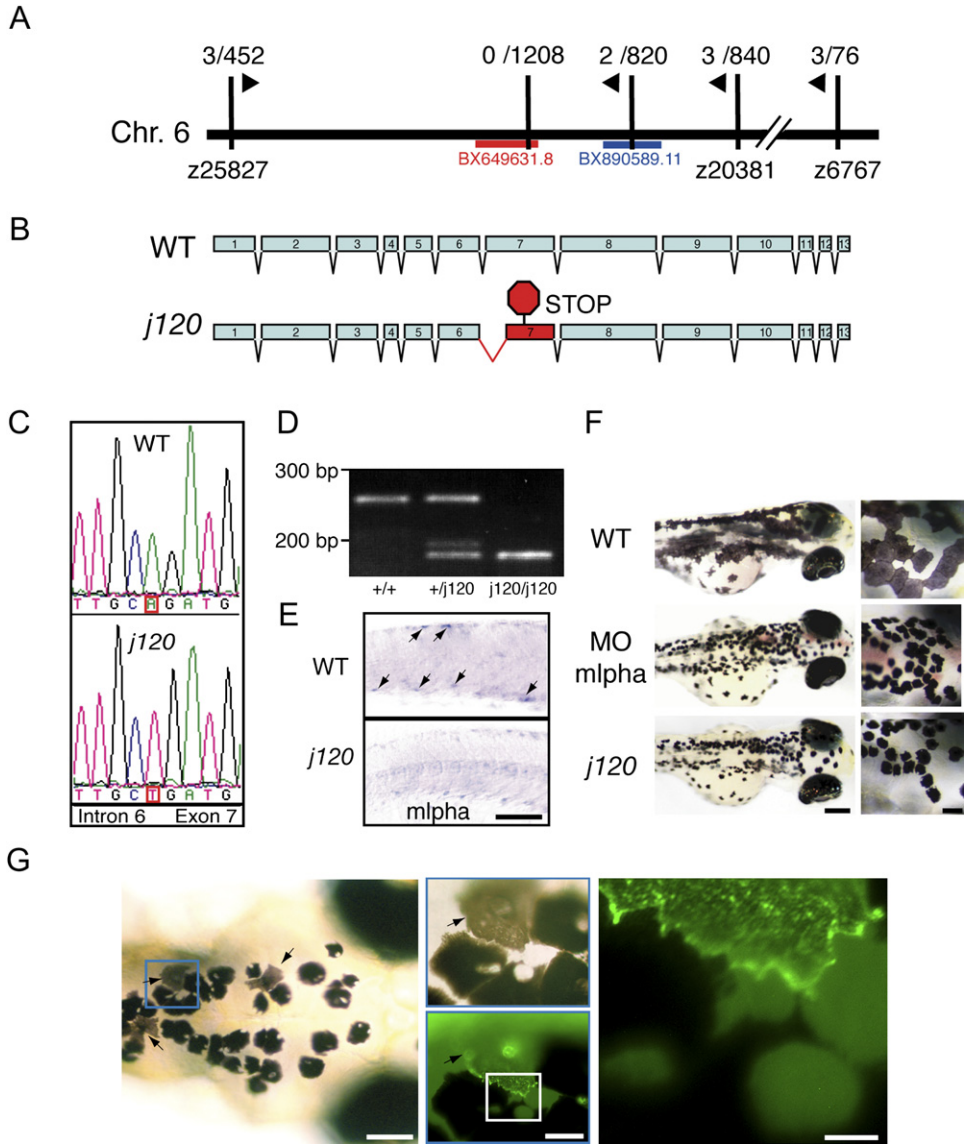


Figure 4. Identification of *j120* as Zebrafish Melanophilin

(A) Linkage of *j120* to SSR markers (vertical black lines) on chromosome 6. The fractions are the observed recombination rates between the mutation and that marker. Zebrafish BAC clone BX649631 contains *mlpha*.

(B) Intron-exon organization of the wild-type and *j120* alleles of the zebrafish *mlpha* gene. A mutation in the *j120* allele leads to abnormal splicing of exon 7, which in turn introduces a stop codon in the coding sequence.

(C) Genomic DNA sequence of wild-type and *j120* alleles of *mlpha* at the junction of intron 6 and exon 7. The mutant has an A-to-T mutation in the predicted splice acceptor site of intron 6.

(D) RT-PCR analysis of *mlpha* exon 7 with RNA from wild-type larvae (+/+) and larvae homozygous (j120/j120) or heterozygous (+/j120) for the *mlpha*$^{j120}$ allele. Gel electrophoresis of the PCR products corresponding to exon 7 shows that only RNA from larvae with the mutant allele yields the shorter PCR product. RNA from homozygous mutant larvae yields only the shorter fragment and not the longer one. Normal and abnormal splicing of exon 7 predict PCR products of these sizes.

(E) In situ hybridization with an antisense probe against *mlpha* mRNA performed on wild-type and homozygous *j120* mutant 2-day-old embryos. Arrows indicate expression in wild-type melanocytes. (The scale bar represents 100 μm.)

(F) Knockdown of Mlpha expression in 3-day-old wild-type larvae. Wild-type embryos were injected with a morpholino antisense (middle panel) or a control oligonucleotide (top panel). Larvae that received the antisense oligonucleotide have contracted pigment, which phenocopies the appearance of pigment in *j120* mutant fish (bottom panel). (Scale bars represent 200 μm in main images and represent 50 μm in insets).

(G) Mosaic rescue in 5-day-old *j120* mutant larvae injected at the one-cell stage with a plasmid containing Mlpha cDNA fused with GFP. Arrows indicate rescued melanocytes. As shown in insets, a GFP-Mlpha expressing melanocyte (arrow) has even dispersion of melanosomes compared to the contracted melanosomes of adjacent melanocytes (Scale Bars, from left to right, represent 100 μm, 25 μm, and 15 μm). The strong particulate fluorescence in the rescued cell suggests that melanosomes recruit GFP-Mlpha.

that the misspliced mRNA is evident in fish homozygous and heterozygous for the mutation but not in wild-type fish (Figure 4D). Premature stop codons often lead to mRNA degradation through nonsense-mediated decay [21], which would create a null. To address this possibility, we used in situ hybridization to evaluate *mlpha*

mRNA expression in 2-day-old embryos (Figure 4E). *mlpha* mRNA staining is conspicuous in the melanocytes of wild-type embryos, as expected for a gene product involved in melanosome transport. Staining is weak in *j120* mutant embryos, and such a finding is consistent with the possibility that the mutation leads to degradation of the mRNA.

To address whether a mutation in *mlpha* can account for the *j120* mutant phenotype, we knocked down expression of *mlpha* mRNA in wild-type embryos with a morpholino antisense oligonucliotide targeting the translation initiation site of *mlpha*. This faithfully phenocopies the *j120* mutant pigment defect (Figure 4F).

Finally, to address whether the *j120* phenotype is solely due to a mutation in *mlpha*, we injected cDNAs encoding either Mlpha or GFP-Mlpha into one-cell *mlpha*$^{j120}$ mutant embryos. Each plasmid contained a melanocyte-specific promoter for controlling transcription [22]. Mosaic expression is a common feature of transient transgenics in zebrafish [23]; and accordingly, we observe a mosaic pattern of rescued melanocytes in those *j120* mutant larvae that had been injected as embryos (Figure 4G; Table 3). The rescued melanocytes in the *j120* mutants are highly conspicuous because they appear much larger than most melanocytes in the mutant, and they are gray instead of black (Figure 4G). This is because their melanosomes are distributed evenly throughout the entire cell. Furthermore, the rescued melanocytes in mutants injected with cDNA encoding GFP-Mlpha appear bright green and when viewed at high magnification, the bright green fluorescence has a granular pattern suggesting that the GFP-Mlpha is enriched on melanosomes (Figure 4G, inset). In contrast to mutants injected with cDNAs encoding Mlpha or GFP-Mlpha, uninjected mutants or mutants injected with plasmid containing GFP alone were never observed to have large, gray melanocytes (Table 3). These rescue and morpholino experiments, together with the molecular analyses of *j120* mutants, establish that the phenotype of partial melanosome dispersion is due to a mutation in zebrafish *mlpha.*

We used bioinformatics to establish that *mlpha* is actually the ortholog of mammalian melanophilin. Melanophilin is a member of the synaptotagmin-like protein (Slp) family, whose members are marked by a conserved N-terminal domain that interacts with GTP-activated Rab27a [19]. We analyzed the phylogenetic relationships between *mlpha*, its predicted zebrafish paralog *mlphb*, and the known mammalian Slp family members (Figure 5A). This indicates zebrafish *mlpha* and *mlphb* are both orthologs of mammalian melanophilin (Figure 5A). Another indication that *mlpha* and mammalian melanophilin are orthologs is that the organization of their introns and exons in the region encoding the Rab27a-binding domain are similar (data not shown). Synteny confirms that zebrafish *mlpha* is orthologous to the mouse and human melanophilin genes: All three genes are proximal to leucine rich repeat (in FLII) interacting protein 1 (LRRFIP1).

Zebrafish chromosomes 6 and 9 are syntenic in the regions that contain *mlphb* and *mlpha*, respectively, implying that *mlpha* and *mlphb* arose from the duplication of a chromosome segment. This is common in the zebrafish genome [24], and many genes present in single copy in mammals have two copies in zebrafish. Virtually nothing is known about the expression or function of *mlphb*. Because it does not compensate for the loss of *mlpha*, its function is not directly relevant to our conclusions about *mlpha*.

Table 3. Fraction of *mlpha*$^{j120}$ Mutant Larvae that Display a Mosaic Pattern of Melanocytes

| cDNA Injected | Concentration (ng/μl) | Number of Mosaic Larvae, Number of Total Larvae Observed |
|---|---|---|
| None | 0 | 0, >1000 |
| GFP | 100 | 0, 13 |
| Mlpha | 50 | 2, 33 |
| Mlpha | 100 | 5, 16 |
| GFP-Mlpha | 100 | 8, 32 |

After injection of the indicated cDNAs into *mlpha*$^{j120}$ mutant embryos on day 0, the larvae were observed in Tricaine at 5 days. Tricaine causes all melanocytes in wild-type larvae to fully disperse their melanosomes (see Figure S1). Melanocytes with dispersed melanosomes (see Figure 4G) were never observed in uninjected mutant larvae or in mutant larvae injected at day 0 with cDNA encoding GFP alone.

To shed light on whether Mlpha and its mammalian ortholog, melanophilin, are functionally similar, we compared their amino acid sequences (Figure 5B) because according to the current model, which is based on studies of the mammalian protein, melanophilin's function is reflected in its amino acid sequence. If the functionally important residues and domains were conserved in Mlpha, this would suggest that the functions of the zebrafish and mammalian proteins are related.

The current model, based on mouse genetics, is that mammalian melanophilin's principal function is to link myosin Va to melanosomes. This is thought to facilitate the transfer of melanosomes from microtubules to cortical actin within the melanocyte dendritic tip, which is where the melanosomes accumulate prior to being taken up by the keratinocyte [18, 25, 26]. This ability of mammalian melanophilin to link myosin Va to the melanosome membrane depends on two protein-interaction domains: an N-terminal domain that binds the activated form of the membrane-anchored, GTP-binding protein, Rab27a [18, 27], and a centrally placed domain that binds myosin Va [18, 25, 28]. Within each domain are particular residues that are highly conserved and functionally crucial (Figure 5B). One of these is R35 in the Rab-27a-binding domain which, when mutated in humans, causes Griscelli syndrome type 3 [20]. Other crucial residues are E380 and E381 in the myosin-Va-binding domain, which are essential for myosin Va recruitment to melanosomes in mammals [28]. In addition, the mammalian melanophilin C terminus contains a predicted coiled-coil region that enhances the binding of melanophilin to myosin Va in mouse melanocytes [25, 28]. Although the amino acid identity between Mlpha and the mouse or human orthologs is only 33% and 37% overall, the residues crucial for Rab27a and myosin Va binding are conserved, as is the predicted C-terminal coiled-coil (Figure 5B). The presence in Mlpha of these conserved residues and structures suggests that Mlpha links myosin V to the melanosome membrane, as in mammals.

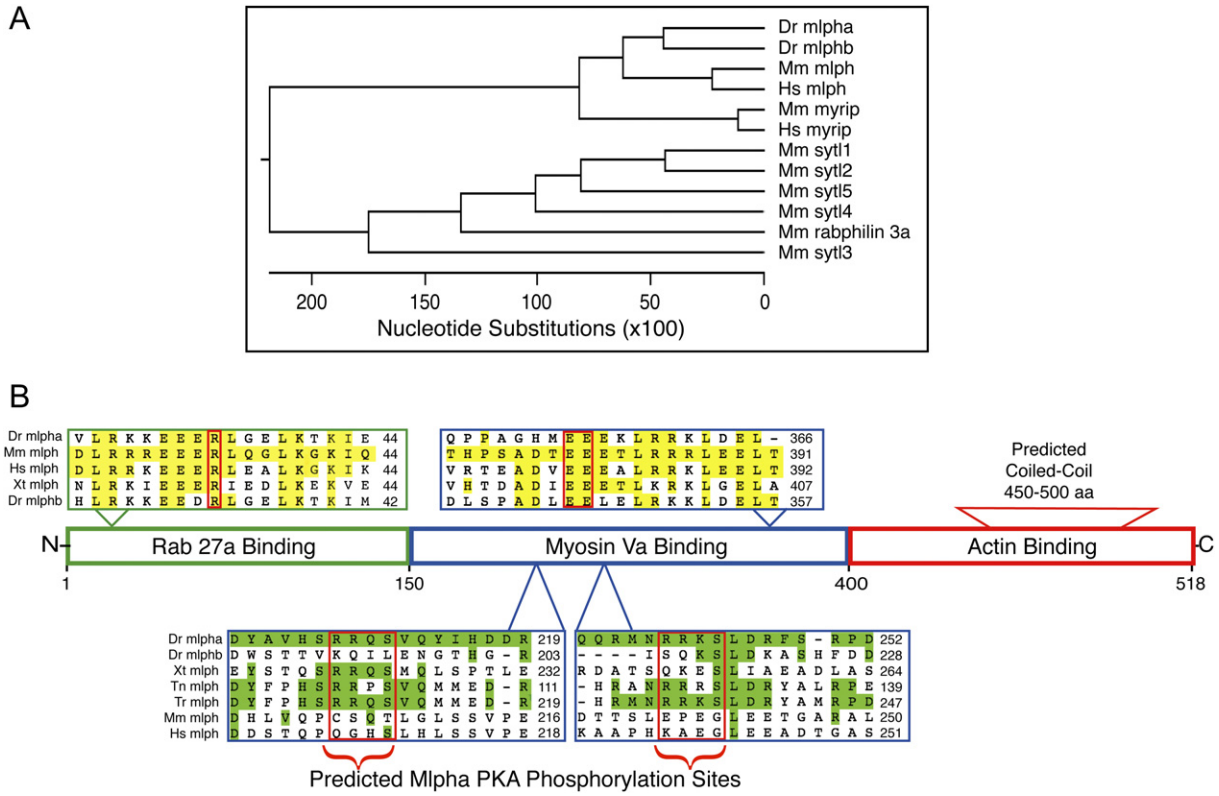


Figure 5. Relationship of *mlpha* and Its Protein Product to Homologs in Other Species

(A) Phylogenetic relationships among members of the synaptotagmin-like protein family. Among the many different members of this family known in humans (Hs) or mouse (Mm), zebrafish (Dr) Mlpha is most closely related to melanophilin (mlph). A second predicted melanophilin gene (*mlphb*) in zebrafish arose through gene duplication.

(B) Alignments of fish, *Xenopus*, mouse, and human melanophilins. Between the upper and lower sequence alignments is a domain map of melanophilin, as established in studies of the mammalian ortholog. Shown in the top portion is the alignment of sequences required for Rab27a and myosin Va binding in mouse (Mm), zebrafish (Dr), human (Hs), and *Xenopus tropicalis* (Xt). Yellow highlights residues that match the mouse sequence. The red boxes outline a conserved and functionally crucial Arginine within the Rab27a binding domain and a tandem pair of conserved and functionally critical glutamate residues (EE) in the myosin Va binding domain. Shown in the bottom portion is the alignment of sequences that include two regions containing predicted PKA phosphorylation sites in Mlpha (outlined in red). Green highlights residues matching zebrafish Mlpha. The predicted PKA phosphorylation sites are conserved in *Xenopus tropicalis* and two other fish species (*Takifugu rubripes* and *Tetraodon nigroviridis*) but not in human, mouse, or zebrafish Mlphb, which is a paralog of Mlpha.

Unlike the mammalian orthologs, the Mlpha amino acid sequence reveals two predicted PKA phosphorylation sites within the myosin V binding domain: $RRQS_{211}$ and $RRKS_{244}$ [29, 30] (Figure 5B). These are present in the melanophilin orthologs of other poikilotherms, including the frog *Xenopus tropicalis* and the fish *Takifugu rubripes* and *Tetraodon nigroviridis*, but absent from mammalian melanophilins (Figure 5B). Thus, these sites are conserved in species such as zebrafish, whose melanocytes engage in rapid, cAMP-dependent changes in pigmentation, but not in mammals, which lack this type of pigmentation control [31]. This correlation is consistent with the possibility that the phosphorylation state of these sites in Mlpha might be important for transducing intracellular cAMP levels into changes in the activities of the melanosome-associated motor proteins (Figure 6). However, there is as yet no evidence that these sites are functional.

## Discussion

The goal of this study was to shed light on how cytoplasmic motor proteins are regulated in vivo. We chose to investigate the problem in fish melanocytes, a well-known paradigm of transport regulation, but with the new idea of using zebrafish for its genetics. We identified the pigmentation mutant allele $mlpha^{j120}$ on the basis of its phenotype: Melanosome dispersion in this mutant is slow and incomplete. We demonstrated that this phenotype is cell autonomous, downstream of cAMP signaling, and independent of actin filaments. Through analyses of individual melanosomes tracks, we determined that the mutant fails to suppress minus-end travel during dispersion, and such a result is consistent with the phenotype of slow and partial melanosome spreading globally. Thus, we provide strong evidence that in zebrafish, melanophilin (Mlpha) has a novel actin-independent role in regulating dynein-dependent melanosome movements early in dispersion. We predict that later in dispersion, Mlpha has a second function, the one it is known for [26], which is to link melanosomes to actin via myosin V (Figure 6). This prediction is based on previous studies of mammalian melanophilin [26], on the conservation of Rab27 and myosin V interaction sites in Mlpha (Figure 5B), and on the colocalization of Mlpha and melanosomes (Figure 4G).

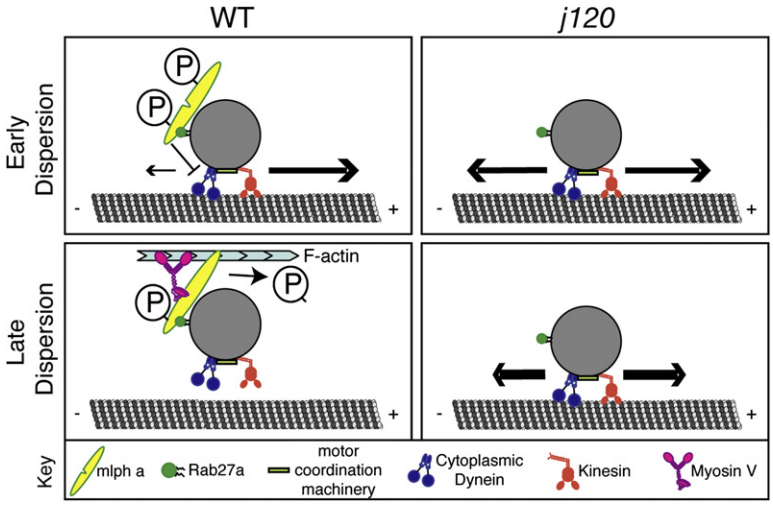


Figure 6. Model of Mlpha Function during Melanosome Dispersion

Model of melanosome dispersion in wild-type melanocytes (left). During the early phase of dispersion, when cAMP levels are high, Mlpha suppresses cytoplasmic dynein. This leads to rapid and global outward movement of melanosomes through the action of the kinesin motor. Later in dispersion, as cAMP levels decline, Mlpha recruits myosin V, which leads to the transfer of melanosomes from microtubules to actin filaments. We note that the myosin V and Rab27a binding sites in Mlpha are predicted but not yet proved on the basis of experimental data. We hypothesize that the dual functions of Mlpha during dispersion may be modulated by changes in the level of PKA phosphorylation, with maximal phosphorylation early in dispersion and declining phosphorylation later. The proposed role for PKA phosphorylation is a hypothesis: There are presently no experimental data on whether the predicted PKA sites in Mlpha are functional. We refer to our proposal that Mlpha implements the transfer of melanosomes from microtubules to actin by coordinating both microtubule- and actin-based transport as a "relay" model. Shown on the right is a model of melanosome dispersion in mlpha$^{j120}$ mutant melanocytes. In the absence of Mlpha, dynein-driven movements are not suppressed in response to the cAMP increase that signals the onset of melanosome dispersion; nor are the melanosomes transferred to actin filaments later on. The average plus- and minus-end travel of melanosomes remains balanced.

Our identification of the mutant allele *j120* as *mlpha*, an ortholog of mammalian melanophilin, initially seemed paradoxical. The zebrafish *mlpha* mutant phenotype involves defective regulation of microtubule-based transport and is independent of actin (Figure 2). Yet in the current model, which is based on studies of mammalian melanocytes, of melanophilin's function, melanophilin is an organelle-associated receptor for myosin V and thereby regulates actin-based transport [26]. The amino acid residues responsible for this function are conserved in Mlpha, hence the paradox: If Mlpha's sole function were to attach myosin V to melanosomes, the mutant would hyperdisperse its melanosomes to the cell margin, similarly to wild-type melanocytes treated with latrunculin (Figure 2B). Instead the mutation slows and spatially limits dispersion through a failure to suppress minus-end travel on microtubules.

To reconcile the apparent discrepancy between Mlpha's presumed function as a myosin V receptor and our experimental finding that the *mlpha* mutant phenotype involves misregulation of dynein and is independent of actin, we invoke a previous study of black tetra fish [9]. Rodionov et al. [9] quantified the microtubule- and actin-based components of melanosome transport over time during dispersion and thereby demonstrated that dispersion proceeds in two phases: an initial period of microtubule-based transport followed by a period of increasing actin-based transport. We propose that the *mlpha*$^{j120}$ mutation interferes with the earlier microtubule-based period and that because of this, the later actin-based phase does not occur. Therefore, treatments that would disrupt the later actin-based phase in wild-type melanocytes, e.g., latrunculin, have no effect on dispersion in the mutant. The fact that wild-type zebrafish melanocytes disperse their melanosomes evenly implies that the initial phase of microtubule-based transport is short relative to the later phase of mixed microtubule- and actin-based transport. The previous study of black tetra melanocytes supports this prediction [9].

The finding that Mlpha regulates microtubule-based transport independently of actin (Figure 2B) is very significant. Were it not for the observation that the *j120* mutant phenotype is unaffected by latrunculin-induced actin disassembly, the failure of the mutant to suppress dynein could have been interpreted as an indirect consequence of disrupting the (putative) myosin V-melanosome linkage function of Mlpha. This alternative explanation of the mutant phenotype, now excluded, would have been based on studies of black tetra fish and frog melanocytes. These studies suggest that minus-end travel episodes are shortened by the tension exerted on the melanosome when myosin V walks on actin [7, 9]. Our findings do not exclude the possibility that myosin V activity also contributes to suppressing dynein motility in wild-type melanocytes. However, this mode of suppression would be in addition to the more direct, actin-independent dynein regulation that we describe in this report (Figure 6).

Our conclusion that early in dispersion Mlpha regulates dynein-dependent melanosome movements and our prediction that later in dispersion it links melanosomes to actin via myosin V raise the question of how these dual functions of Mlpha are regulated temporally. Our working model is that the phosphorylation state of the predicted PKA sites in Mlpha might change with the rise and fall of cAMP during dispersion and that this may orchestrate the switch from dynein-driven transport to myosin V-driven transport (Figure 6). This hypothesis is based on melanophilin sequence comparisons between different species (Figure 5B), wherein the presence of predicted PKA sites correlates with the property of rapid cAMP-dependent pigmentation control. In addition, our proposal that Mlpha switches between dynein regulator and myosin V recruiter depending on the status of its putative PKA phosphorylation sites fits very well with the findings of a previous study of black tetra fish [9]. Their study reported that dispersion involves predominantly microtubule-based transport

initially, that the levels of actin-based transport then increases with time, and that these two phases are regulated temporally by the level of cAMP. Therefore, the findings and model of Rodionov et al. [9] fit very well with our identification of Mlpha as a dynein regulator, the functions we propose for Mlpha's predicted cAMP dependent phosphorylation sites, and Mlpha's predicted Rab27 and myosin V binding activities. For testing this model, it will be important to address whether all of these predicted sites in Mlpha are functional.

Previous studies of melanophilin or related members of the Slp family that have analogous functions in other types of cells e.g., MyRIP [32] and rabphilin 3a [33, 34], have not addressed the possibility that proteins in this family also regulate microtubule-based transport in addition to their functions of linking myosins to organelle-bound Rab proteins. The central new idea provided by our study is that the transfer of melanosomes from microtubules to actin might involve more than simply attaching the myosin to the organelle and allowing the myosin to rip the organelle off the microtubule during dynein-driven motility episodes [7]. In contrast to this "tug-of war" model, wherein the attachment of myosin V to the organelle alone determines how far the organelle travels along the microtubule, our findings raise the possibility of a "relay model" wherein travel along the microtubule is regulated in a separate step that precedes recruitment or activation, or both, of myosin V. Our finding that a single protein, Mlpha, regulates melanosome travel along the microtubule and in addition might link myosin V to the melanosome supports this model.

This study raises several questions that will need to be addressed through future work. Does Mlpha actually link myosin Va to melanosomes, as suggested by Mlpha's amino acid sequence? Within Mlpha, what is the domain that is responsible for suppressing dynein-driven motility? Are the predicted phosphorylation sites in Mlpha functional, and does their phosphorylation state regulate microtubule- and actin-based transport, as proposed in the hypothesis of Figure 6? Addressing these questions will help define the mechanism of dynein regulation during dispersion and shed light on whether this function is retained in the mammalian ortholog.

## Experimental Procedures

### Fish Stocks and Mutagenesis

WIK, AB, and TU lines were obtained from the Zebrafish International Resource Center (ZIRC). ENU mutagenesis was performed as described previously [35].

### Larvae Melanosome-Transport-Screening Assay

We sedated 5-day-old larvae with a mixture of 200 ppm quinaldine and 0.1 mg/ml lidocaine in E3 solution (5 mM NaCl, 0.17 mM KCl, 0.33 mM $CaCl_2$, and 0.33 mM $MgSO_4$). We avoided the sedative Tricaine because it elicits melanosome dispersion in larvae (Figure S1). After exposing the larvae for 10 min to 5 μM MCH (Bachem, King of Prussia, PA) diluted in sedative solution containing 0.1% DMSO, we examined them for aggregation defects. After this, we incubated the same larvae in 10–30 μM MSH (Sigma-Aldrich, St. Louis, MO) for 10–20 min and then screened them for dispersion defects. We observed larvae under brightfield by using a Leica MZFLII stereomicroscope equipped with a 1.0× PlanApo lens (Leica Microsystems, Wetzlar, Germany). Digital photos were taken with a Magnifire-SP digital camera (Optronics, Goleta, CA).

### Primary Melanocyte Cultures

Prim 5 stage (24 hr) embryos were bleached and dechorionated [36], and at 5–7 days of age, the larvae were anesthetized and dissociated in ice-cold calcium-free Ringers solution (116 mM NaCl, 2.9 mM KCl, and 5 mM HEPES [pH 7.2]). Dissociated tissue was rinsed three times in 50 ml sterile calcium-free Ringers and incubated in 0.05% trypsin solution with EDTA (Invitrogen, Carlsbad, California) for 20 min at room temperature. The cells were centrifuged, and the cell pellet rinsed with L-15 media (Cellgro, Mediatech, Herndon, VA) supplemented with 10% FBS, 0.2% gentamycin, 0.5% penicillin, 0.5% streptomycin (Invitrogen, Carlsbad, CA), and 0.8 mM $CaCl_2$ 1M $CaCl_2$. The cell pellet was then resuspended in the culture media to a density of 125,000–500,000 $ml^{-1}$, and this cell suspension was then plated onto clean glass 25 mm diameter No. 1 coverslips (Fisher Scientific, Hampton, NH) that had been coated with a mixture of 20 μg/ml laminin and 10 μg/ml fibronectin (Roche, Basel, Switzerland) or 0.2 mg/ml E-C-L (Upstate, Charlottesville, VA). Approximately 0.25 ml of cell suspension was incubated with each coverslip for 4–8 hr. After plating, each coverslip was cultured at room temperature for up to 2 weeks in 2.5 ml of L15 media containing the supplements listed above.

### Imaging Cultured Melanocytes

Coverslips with attached cells were sealed into a microscope flow chamber (Model RC-21BR, Warner Instruments, Hamden, CT) and bathed with Ringers solution (116 mM NaCl, 2.9 mM KCl 5 mM, HEPES [pH 7.2], and 1.8 mM $CaCl_2$). Cells were imaged by differential interference contrast or by bright field with a Zeiss Axioplan microscope (Zeiss, Oberkochen, Germany) equipped with a custom fiber-optic illuminator coupled to a Hg arc lamp. We used the following Plan-Neofluor oil immersion objectives: 40× (N.A. = 1.3); 100× (N.A. = 1.3). Digital images were acquired with a Photometrics CoolSNAP CCD camera (Roper Scientific, Trenton, NJ) and stored on a personal computer, all under the control of MetaMorph imaging software (Molecular Devices Corporation, Sunnyvale, CA).

For evaluation of the organization of the melanocyte microtubule and actin cytoskeletons, cultures were fixed with 4% paraformaldehyde in 1× PBS, immunostained with a primary antibody against α-tubulin (Sigma-Aldrich), and labeled with rhodamine phalloidin (Molecular Probes, Invitrogen). Fluorescent cells were observed with epi-illumination with the 40× oil-immersion objective and either FITC or rhodamine filter sets from Chroma (Rockingham, VT). Digital images were processed with MetaMorph and Adobe Photoshop software.

### Pharmacological Studies of Cultured Melanocytes

The following reagents (from Sigma-Aldrich unless otherwise noted) were diluted in Ringers and perfused into the microscope chamber: 0.1–10 μM MCH (Bachem), 0.2–20 μM MSH, 0.01 mM epinephrine, 5 mM caffeine, 200 μM forskolin, 0.1–1 mM SQ 22536, 40 μM H-89, 30 μM sp-cAMP, 0.5–10 μM okadaic acid, and 5 μM latrunculin A. Melanocytes in culture media were preincubated with okadaic acid overnight prior to exposure to MCH or epinephrine.

### Quantitation of Global Melanosome Dispersion

Immediately after drug application, digital images of individual melanocytes were collected for a period of 5–10 min with a camera exposure time of 150 ms. To plot the time course of global melanosome dispersion, we used Metamorph software to trace the perimeter of the cell in the first frame and to compute the enclosed "projected cell area," which did not change with time during dispersion. A threshold applied to each frame in a given sequence isolated the pixels occupied by melanosomes, and the summed projected area of the melanosomes was divided by the total projected cell area for computation of the percent of the cell area filled by melanosomes. The fractional cell area occupied by melanosomes in successive frames was plotted against time.

### Single-Melanosome Tracking during Dispersion

Initial exposure of melanocytes to MCH or epinephrine brought about the aggregation of their melanosomes. They were then stimulated with 5 mM caffeine or 5 μM MSH so that dispersion could be initiated. At 1.5 and 3 min after dispersion initiation, images were captured at three frames per second with an exposure time of 150

or 300 ms exposure. The vast majority of image sequences lasted 30 s. Individual melanosomes were tracked with the centroid-tracking function provided by MetaMorph software. The method's spatial precision was determined from the distribution of a single melanosome's positions within a paraformaldehyde-fixed cell (mean = 2.7 nm; SD = 3.8 nm; n = 657 frames).

Melanosome tracks were manually decomposed into three motion categories: linear outward (plus-end) movement, linear inward (minus-end) movement, and episodes of nondirected movement or pause (Figure 3). Linear melanosome displacement was defined as a displacement that was away from or toward the cell center and that was greater than 30 nm within an interval of 300 ms. The endpoint of a linear run was determined by a pause or reversal of movement along the microtubule axis. Pauses were defined as episodes wherein melanosome displacement was less than 30 nm over 300 ms. Periods of random motion were defined as episodes where the melanosome's displacement was greater than 30 nm over 300 ms and did not appear to fall along a line or lines for at least 900 ms. Most random motion episodes lasted much longer than 300 ms. To measure run lengths associated with linear travel along microtubules, we used the least-squares method to compute the best fit line to the trajectory and then summed the components of the motion along this line.

### Positional Cloning and Molecular Analysis of *mlpha*$^{j120}$

We outcrossed *j120/j120* fish in a C32 background with wild-type WK fish to make heterozygous *j120* carriers in a C32/WIK background. These map-cross fish were mated, and their progeny was screened for the *j120* phenotype at 4 to 5 days after fertilization. Screened larvae were fixed in methanol, the genomic DNA was isolated, and PCR reactions were performed with primers that revealed sequence polymorphisms between C32 and WIK at known loci. Linkage to chromosome 6 was established with simple sequence length polymorphisms (SSLPs). Fine mapping was performed with simple sequence repeat (SSR) markers documented in the following databases: The Zebrafish Information Network, http://zfin.org; Tübingen Map of Zebrafish Genome, http://wwwmap.tuebingen.mpg.de; and Zebrafish SSR Search, http://danio.mgh.harvard.edu/markers/ssr.html.

To sequence genomic DNA, we PCR amplified and sequenced overlapping fragments of the *mlpha* gene, by using information from the Zebrafish Genome-Sequencing Project (www.ensembl.org/danio_rerio/index.html) to design the PCR and sequencing primers. To make *mlpha* cDNA, we isolated mRNA by using the (Poly(A)Purist Kit (Ambion, Austin, TX) and then performed RT-PCR by using the Advantage RT for PCR kit (BD Biosciences, San Jose, CA). The PCR primers for cloning the Mlpha protein coding sequence were 5′-TCCTGAAAGACTTGGCAACTG-3′ and 5′-CGTCTTTATGCCAGTCTGTCAAA-3′. The primers for amplifying a 251 bp fragment that contains the premature stop codon in the mutant were 5′-TCACTCTCGCAGACAGTCTGT-3′ and 5′-TCTACCTGGACACTTCAGAGGAAGAGGATA-3′. To identify the point mutation in *j120*, we amplified the genomic DNA with the primers 5′-GAAGAAAATATATTAGGAAATACGGT-3′ and 5′-CATCACTGATTAAGGCGCTTTA-3′.

### In Situ Hybridization

Whole-mount in situ hybridization was performed with larvae treated with 0.003% PTU [37] at 24 hr, 48 hr, 3 days, and 4 days after fertilization. Digoxigenin-labeled antisense RNA probes were synthesized with linearized plasmid DNA containing zebrafish melanophilin as the template (Open Biosystems, clone ID 8008178).

### Morpholino Injection

Morpholino oligonucleotides (Gene Tools, Philomath, OR) were dissolved in distilled water, diluted to 1 mM in 1× Danieau solution (58 mM NaCl, 0.7 mMKCl, 0.4 mM $MgSO_4$, 0.6 mM $Ca(NO_3)_2$, and 5.0 mM HEPES [pH 7.6]), and injected into one- to two-cell wild-type embryos with 0.05% phenol red as a marker. The sequence of the melanophilin morpholino was 5′-GACAGGTCCAACTTCTTGTCCA TGT-3′. A standard control morpholino (5′-CCTCTTACCTCAGTTAC AATTTATA-3′) was also injected for confirmation that the phenotype observed was not due to toxicity.

### *Rescue*

We made plasmid constructs by inserting full-length Mlpha cDNA, either with or without N-terminally fused GFP, into the BamHI/EcoRI sites of a vector containing the melanocyte specific Mitfa promoter (a gift from James Lister). The plasmids were linearized, diluted to a concentration of 50 or 100 ng/μl, and injected into one-cell stage embryos. The 5-day-old larvae were sedated with 0.02% tricaine, which normally disperses their pigment, and examined through a stereo dissection microscope for rescue. For making high-resolution pictures of rescued melanocytes in situ, larvae were imaged with a Zeiss Axio Imager MI microscope (Zeiss) with a Plan-Neofluor 10× (N.A. = 0.3) objective and an Achroplan 63× (N.A. = 0.95) water-immersion objective. Digital images were acquired with a Zeiss Axiocam.

### Supplemental Data

Two figures are available at http://www.current-biology.com/cgi/content/full/17/20/1721/DC1/.

### Acknowledgments

We thank Dr. William Talbot (Department of Developmental Biology, Stanford School of Medicine) for rough mapping *j120* to chromosome 6. We are grateful to Dr. Monte Westerfield (Institute of Neuroscience, University of Oregon) for helpful advice and to Dr. Gary Banker for comments on the manuscript. This work was supported by a grant from the National Institute of Health (B.J.S., R01 GM60045) and by a National Research Service Award predoctoral fellowship (L.S., F31 GM071198).

Received: March 12, 2007
Revised: August 1, 2007
Accepted: September 11, 2007
Published online: October 4, 2007

### References

1. Nascimento, A.A., Roland, J.T., and Gelfand, V.I. (2003). Pigment cells: A model for the study of organelle transport. Annu. Rev. Cell Dev. Biol. *19*, 469–491.
2. Rodionov, V.I., Hope, A.J., Svitkina, T.M., and Borisy, G.G. (1998). Functional coordination of microtubule-based and actin-based motility in melanophores. Curr. Biol. *8*, 165–168.
3. Reilein, A.R., Serpinskaya, A.S., Karcher, R.L., Dujardin, D.L., Vallee, R.B., and Gelfand, V.I. (2003). Differential regulation of dynein-driven melanosome movement. Biochem. Biophys. Res. Commun. *309*, 652–658.
4. Tuma, M.C., Zill, A., Le Bot, N., Vernos, I., and Gelfand, V. (1998). Heterotrimeric kinesin II is the microtubule motor protein responsible for pigment dispersion in Xenopus melanophores. J. Cell Biol. *143*, 1547–1558.
5. Rogers, S.L., and Gelfand, V.I. (1998). Myosin cooperates with microtubule motors during organelle transport in melanophores. Curr. Biol. *8*, 161–164.
6. Rogers, S.L., Karcher, R.L., Roland, J.T., Minin, A.A., Steffen, W., and Gelfand, V.I. (1999). Regulation of melanosome movement in the cell cycle by reversible association with myosin V. J. Cell Biol. *146*, 1265–1276.
7. Gross, S.P., Tuma, M.C., Deacon, S.W., Serpinskaya, A.S., Reilein, A.R., and Gelfand, V.I. (2002). Interactions and regulation of molecular motors in Xenopus melanophores. J. Cell Biol. *156*, 855–865.
8. Rogers, S.L., Tint, I.S., Fanapour, P.C., and Gelfand, V.I. (1997). Regulated bidirectional motility of melanophore pigment granules along microtubules in vitro. Proc. Natl. Acad. Sci. USA *94*, 3720–3725.
9. Rodionov, V., Yi, J., Kashina, A., Oladipo, A., and Gross, S.P. (2003). Switching between microtubule- and actin-based transport systems in melanophores is controlled by cAMP levels. Curr. Biol. *13*, 1837–1847.
10. Skibbens, R.V., Skeen, V.P., and Salmon, E.D. (1993). Directional instability of kinetochore motility during chromosome congression and segregation in mitotic newt lung cells: A push-pull mechanism. J. Cell Biol. *122*, 859–875.

11. Gunawardena, S., and Goldstein, L.S. (2004). Cargo-carrying motor vehicles on the neuronal highway: Transport pathways and neurodegenerative disease. J. Neurobiol. *58*, 258–271.
12. Allan, V.J., and Schroer, T.A. (1999). Membrane motors. Curr. Opin. Cell Biol. *11*, 476–482.
13. Rozdzial, M.M., and Haimo, L.T. (1986). Bidirectional pigment granule movements of melanophores are regulated by protein phosphorylation and dephosphorylation. Cell *47*, 1061–1070.
14. Sammak, P.J., Adams, S.R., Harootunian, A.T., Schliwa, M., and Tsien, R.Y. (1992). Intracellular cyclic AMP not calcium, determines the direction of vesicle movement in melanophores: Direct measurement by fluorescence ratio imaging. J. Cell Biol. *117*, 57–72.
15. Levi, V., Serpinskaya, A.S., Gratton, E., and Gelfand, V. (2006). Organelle transport along microtubules in Xenopus melanophores: Evidence for cooperation between multiple motors. Biophys. J. *90*, 318–327.
16. Schnapp, B.J., Crise, B., Sheetz, M.P., Reese, T.S., and Khan, S. (1990). Delayed start-up of kinesin-driven microtubule gliding following inhibition by adenosine 5′-[beta,gamma-imido]triphosphate. Proc. Natl. Acad. Sci. USA *87*, 10053–10057.
17. Gross, S.P., Welte, M.A., Block, S.M., and Wieschaus, E.F. (2000). Dynein-mediated cargo transport in vivo. A switch controls travel distance. J. Cell Biol. *148*, 945–956.
18. Wu, X.S., Rao, K., Zhang, H., Wang, F., Sellers, J.R., Matesic, L.E., Copeland, N.G., Jenkins, N.A., and Hammer, J.A., 3rd. (2002). Identification of an organelle receptor for myosin-Va. Nat. Cell Biol. *4*, 271–278.
19. Fukuda, M., Kuroda, T.S., and Mikoshiba, K. (2002). Slac2-a/melanophilin, the missing link between Rab27 and myosin Va: Implications of a tripartite protein complex for melanosome transport. J. Biol. Chem. *277*, 12432–12436.
20. Menasche, G., Ho, C.H., Sanal, O., Feldmann, J., Tezcan, I., Ersoy, F., Houdusse, A., Fischer, A., and de Saint Basile, G. (2003). Griscelli syndrome restricted to hypopigmentation results from a melanophilin defect (GS3) or a MYO5A F-exon deletion (GS1). J. Clin. Invest. *112*, 450–456.
21. Maquat, L.E. (2002). Nonsense-mediated mRNA decay. Curr. Biol. *12*, R196–R197.
22. Lister, J.A., Robertson, C.P., Lepage, T., Johnson, S.L., and Raible, D.W. (1999). nacre encodes a zebrafish microphthalmia-related protein that regulates neural-crest-derived pigment cell fate. Development *126*, 3757–3767.
23. Meng, A., Jessen, J.R., and Lin, S. (1999). Transgenesis. Methods Cell Biol. *60*, 133–148.
24. Postlethwait, J.H., Woods, I.G., Ngo-Hazelett, P., Yan, Y.L., Kelly, P.D., Chu, F., Huang, H., Hill-Force, A., and Talbot, W.S. (2000). Zebrafish comparative genomics and the origins of vertebrate chromosomes. Genome Res. *10*, 1890–1902.
25. Hume, A.N., Tarafder, A.K., Ramalho, J.S., Sviderskaya, E.V., and Seabra, M.C. (2006). A coiled-coil domain of melanophilin is essential for myosin Va recruitment and melanosome transport in melanocytes. Mol. Biol. Cell *17*, 720–735.
26. Li, X.D., Ikebe, R., and Ikebe, M. (2005). Activation of myosin Va function by melanophilin, a specific docking partner of myosin Va. J. Biol. Chem. *280*, 17815–17822.
27. Wu, X., Wang, F., Rao, K., Sellers, J.R., and Hammer, J.A., 3rd. (2002). Rab27a is an essential component of melanosome receptor for myosin Va. Mol. Biol. Cell *13*, 1735–1749.
28. Kuroda, T.S., Itoh, T., and Fukuda, M. (2005). Functional analysis of slac2-a/melanophilin as a linker protein between Rab27A and myosin Va in melanosome transport. Methods Enzymol. *403*, 419–431.
29. Kemp, B.E., and Pearson, R.B. (1990). Protein kinase recognition sequence motifs. Trends Biochem. Sci. *15*, 342–346.
30. Obenauer, J.C., Cantley, L.C., and Yaffe, M.B. (2003). Scansite 2.0: Proteome-wide prediction of cell signaling interactions using short sequence motifs. Nucleic Acids Res. *31*, 3635–3641.
31. Wu, X., and Hammer, J.A., 3rd. (2000). Making sense of melanosome dynamics in mouse melanocytes. Pigment Cell Res. *13*, 241–247.
32. Kuroda, T.S., and Fukuda, M. (2005). Functional analysis of Slac2-c/MyRIP as a linker protein between melanosomes and myosin VIIa. J. Biol. Chem. *280*, 28015–28022.
33. Fukuda, M., Kanno, E., and Yamamoto, A. (2004). Rabphilin and Noc2 are recruited to dense-core vesicles through specific interaction with Rab27A in PC12 cells. J. Biol. Chem. *279*, 13065–13075.
34. Tsuboi, T., and Fukuda, M. (2005). The C2B domain of rabphilin directly interacts with SNAP-25 and regulates the docking step of dense core vesicle exocytosis in PC12 cells. J. Biol. Chem. *280*, 39253–39259.
35. Rawls, J.F., Frieda, M.R., McAdow, A.R., Gross, J.P., Clayton, C.M., Heyen, C.K., and Johnson, S.L. (2003). Coupled mutagenesis screens and genetic mapping in zebrafish. Genetics *163*, 997–1009.
36. Westerfield, M. (2000). The Zebrafish Book. A Guide for the Laboratory Use of Zebrafish (Danio rerio), Fourth Edition (Eugene, OR: Univ. of Oregon Press).
37. Ransom, D.G., Bahary, N., Niss, K., Traver, D., Burns, C., Trede, N.S., Paffett-Lugassy, N., Saganic, W.J., Lim, C.A., Hersey, C., et al. (2004). The zebrafish moonshine gene encodes transcriptional intermediary factor 1gamma, an essential regulator of hematopoiesis. PLoS Biol. *2*, E237.
38. Thaler, C.D., and Haimo, L.T. (1992). Control of organelle transport in melanophores: Regulation of Ca2+ and cAMP levels. Cell Motil. Cytoskeleton *22*, 175–184.